

# Evaluation of Exerting Force on the Heating Surface Due to Bubble Ebullition in Subcooled Flow Boiling

M. R. Nematollahi

**Abstract**—Vibration characteristics of subcooled flow boiling on thin and long structures such as a heating rod were recently investigated by the author. The results show that the intensity of the subcooled boiling-induced vibration (SBIV) was influenced strongly by the conditions of the subcooling temperature, linear power density and flow velocity. Implosive bubble formation and collapse are the main nature of subcooled boiling, and their behaviors are the only sources to originate from SBIV. Therefore, in order to explain the phenomenon of SBIV, it is essential to obtain reliable information about bubble behavior in subcooled boiling conditions. This was investigated at different conditions of coolant subcooling temperatures of 25 to 75°C, coolant flow velocities of 0.16 to 0.53 m/s, and linear power densities of 100 to 600 W/cm. High speed photography at 13,500 frames per second was performed at these conditions. The results show that even at the highest subcooling condition, the absolute majority of bubbles collapse very close to the surface after detaching from the heating surface. Based on these observations, a simple model of surface tension and momentum change is introduced to offer a rough quantitative estimate of the force exerted on the heating surface during the bubble ebullition. The formation of a typical bubble in subcooled boiling is predicted to exert an excitation force in the order of  $10^{-4}$  N.

**Keywords**—Subcooled boiling, vibration mechanism, bubble behavior.

## NOMENCLATURE

ave = average

A = area,  $m^2$

F = force, N

D = diameter, m

FFT = fast Fourier transform

LPD = linear power density,  $\frac{W}{cm}$

$\dot{m}$  = Mass flow rate,  $\frac{kg}{s}$

$\Delta p$  = Pressure difference

$p$  = Pressure

$r$  = radius

SBIV = subcooled-boiling-induced vibration

SMB = stable micro-bubble

$T$  = temperature

TD = temperature dependency

T = time, s

V = volume,  $m^3$

$R$  = gas constant

$v$  = average velocity

$\Delta$  = gradient or difference

$\rho$  = Density,  $\frac{kg}{m^3}$

$\sigma$  = Surface tension,  $\frac{N}{m}$

## SUBSCRIPTS

Cs = control surface

Cv = control volume

e = exhaustion

in = inner

Sub = subcooled

w = water

x = x direction

## I. INTRODUCTION

THE ability of subcooled flow boiling for transferring high heat loading in a compact area without a significant void fraction and a significant increase in heating surface temperature causes this technique to be widely used in industry. Because of the special characteristics of subcooled flow boiling, this technique is used for making compact heat

M. R. Nematollahi is with School of Engineering, Shiraz University, Shiraz, Iran (phone/fax: +98-711-6287500; e-mail: nema@shirazu.ac.ir, mmnema@yahoo.com).

exchangers or transferring high heat loadings in nuclear plants. Using the subcooled boiling technique, transferring heat fluxes of up to  $10^8 \text{ W/m}^2$  are reported to be attainable through high velocities, large subcooling, small diameter channels and short heated lengths [1]. Subcooled boiling from some other related area is also interested for many researchers such as those in [2] and [3].

There are, however, some limitations and problems in the design of such heat exchangers. For example, higher flow velocities cause destructive effects of flow-induced vibrations in small diameter channels and tubes due to the decrease of tube shearing strength. Also subcooled flow boiling itself can cause the vibration of thin and long heating surfaces [4-6]. These problems may cause the vibration-induced failure of heat exchangers, which limits the usage of the full ability of subcooled flow boiling in transferring high heat fluxes.

Subcooled boiling induced vibration of thin and long structures such as heating rods was recently studied experimentally by the author [4-6]. Implosive bubble formation and collapse are the main characteristics of subcooled boiling and distinguish the subcooled boiling regime. It is also the only possible source that can cause the excitation force for the vibration of the heating elements due to subcooled boiling. Therefore, in order to explain the mechanism of subcooled boiling induced vibration (SBIV), it was essential to get reliable information about bubble behavior in subcooled boiling conditions.

The rod vibration can simulate the typical behavior of a fuel rod or a steam generator tube in a nuclear reactor. The history of nuclear power plants operation experience has shown vibration induced rod or tube failure because of FIV or SBIV [12].

In the present study an attempt was made to investigate the mechanisms of SBIV by analyzing bubble behavior in subcooled flow boiling on a heated rod using the technique of high-speed photography. The bubble behavior at three locations at 1, 25 and 45 cm from the beginning of a heated rod were analyzed at different conditions of subcooling temperature, linear power density and flow rate. A simple form of the exciting force due to bubble formation and collapse is reported in this article. A model based on surface tension and momentum transfer is introduced to explain the character of the exciting force during the bubble growth. Note that the bubble behavior in boiling is completely different with those in cavitations; therefore their force effect mechanisms are also completely different.

## II. BACKGROUND

It appears that research works on the vibration aspects of subcooled boiling are very rare and are mostly concerned with the effect of the external vibration of the heating surface on the enhancement of the heat transfer rate [7-8], or with the thermo-acoustic phenomena of subcooled boiling that can yield detection of subcooled boiling heat transfer regimes [9]. Also detection of subcooled boiling heat transfer regimes by

accelerometer equipment up to critical heat flux are addressed by G.P. Celata et al. [10] and that for different heat transfer regimes has expressed by the author et al. [11].

Vibration problems have become increasingly important in recent years as structures have been progressively made lighter and more flexible, but more prone to vibration. This is so materials can be used near their mechanical limits. Therefore, the vibration-induced failure of such systems involving fluid flow with boiling or subcooled boiling heat transfer conditions has become one of the most critical issues to be addressed.

An experimental investigation on SBIV was reported in past few years by the author [4-6]. In this work, a subcooled boiling loop with an annular flow configuration on an electrically heated rod was used to measure the induced vibration due to subcooled boiling at different subcooling temperatures, linear power densities and flow rates by a mono-axial accelerometer attached to the rod (see Fig. 1). A summary of the significant results of this study on the vibration characteristics of subcooled flow boiling instability is presented in the following.

The results show that, in spite of several damping mechanisms in the system, the SBIV intensity was strong enough to be measured even in the presence of the FIV [5]. The results also indicate that the intensity of SBIV is influenced strongly by the conditions of the subcooling temperature, linear power density and flow rate. Fig. 2 shows the results of the temperature dependency (TD) test of two different experimental runs [12]. In this figure, the mono-axial measured acceleration is normalized with the earth gravitational acceleration. In order to have a scale for the intensity of the rod vibration in the TD test, the intensity of the rod vibration without heat generation is also presented in this figure. This figure shows relatively good data reproducibility over the entire range of subcooled temperature. It is found that despite damping mechanisms installed in the apparatus for the rod vibration, there are intensive vibrations caused by subcooled boiling when the inner subcooled temperature of the coolant is relatively high ( $\Delta T_{\text{sub}} > 35 \text{ K}$ ). The effect of subcooled boiling on the rod vibration is reduced when the coolant temperature approaches the saturated temperature ( $\Delta T_{\text{sub}} < 30 \text{ K}$ ). Nonetheless, even in low subcooling conditions the vibration intensity is several times stronger than in the case without any heat generation (see the pump background vibration intensity and power spectral density in Fig. 2 and Fig. 3-b, respectively).

The Fast Fourier Transform (FFT) results of the natural frequency, the background and the temperature dependency of SBIV shown in Fig. 3. The natural frequency test indicated that the two most possible natural frequencies of the rod (shown in Fig. 3-a) are around 30 Hz and 125 Hz in a frequency range between 0~500 Hz. However there are some frequencies around 200 Hz that have also showed weak excitation. Fig. 3-c and Fig. 3-d indicate that the system generally shows high levels of power spectral in the entire range of recorded frequency (0 to 1000 Hz) when subcooled

boiling is present. In other words, SBIV does not contain any special vibration frequency. However, the natural frequency of the rod is more excited at some range of subcooled temperatures such as 40 and 80 K in comparison to their neighborhood temperatures.

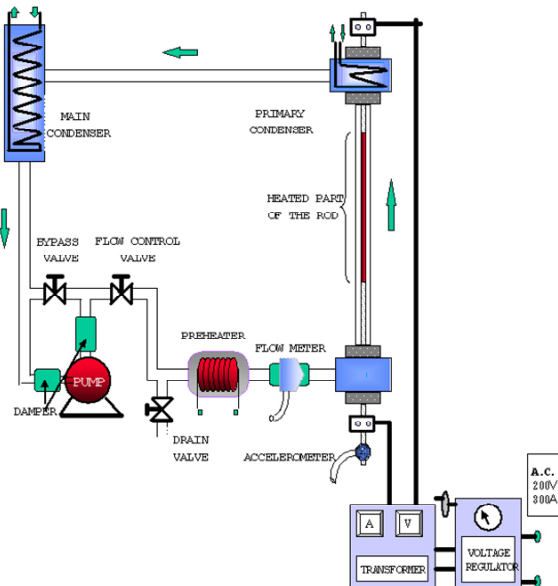


Fig. 1 Schematic diagram of the experimental setup

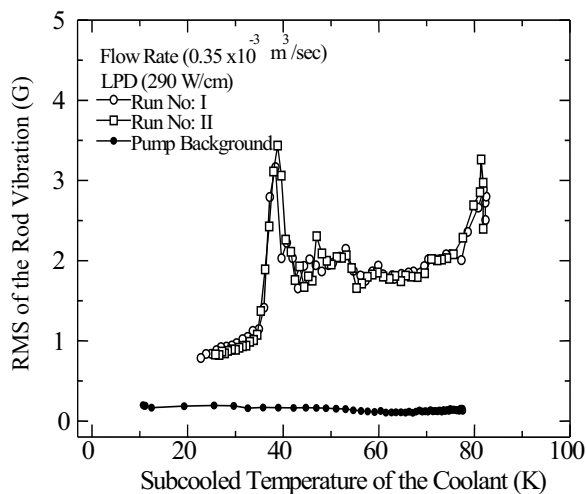
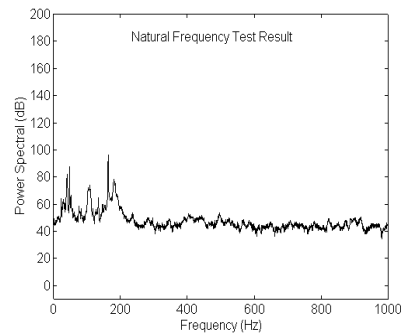
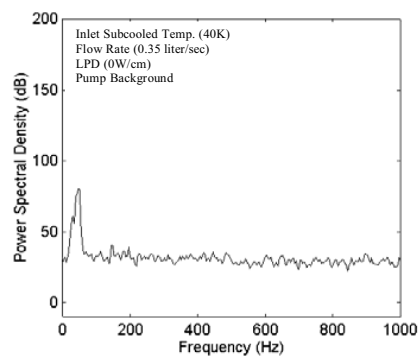


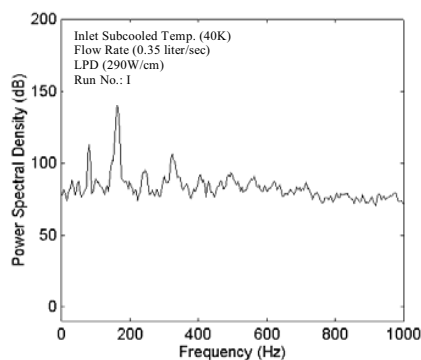
Fig. 2 Results of two different runs of temperature dependency test of SBIV



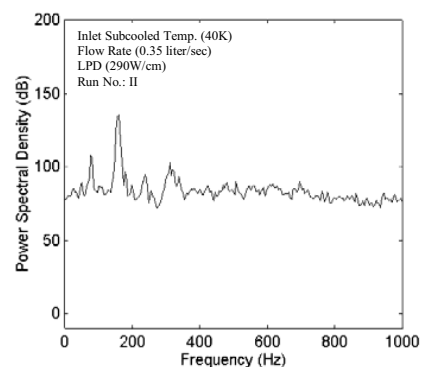
(a)



(b)



(c)



(d)

Fig. 3 Comparing of power spectral density due SBIV

### III. EXPERIMENTAL APPARATUS AND PROCEDURE OF HIGH-SPEED PHOTOGRAPHY

Fig. 1 shows a schematic view of the test loop. Subcooled boiling occurs by Joule heating on the middle part of a stainless steel rod that has a high electrical resistance compared to the rest of the rod which is made from copper. The flow of distilled water is used as the re-circulating coolant in the loop. A power between 0 to 60 kW is supplied from a voltage regulator and a transformer which was connected to the power line. The rod diameter is 10 mm, and the length of the heated surface of the rod is 50 cm. The outer tube of the test section is made of glass (30 mm inner diameter) to allow visual observation.

The experiments are carried out after degassing the primary operation to insure that the effect of the dissolved gasses is ignored, coolant subcooling temperature is at 25 to 75K, there are coolant flow velocities of 0.16, 0.32 and 0.53m/sec, and imposed linear power densities are from 100 to 600 W/cm. High-speed photography was performed using a Kodak Ektapro High-speed Motion Analyzer (model 4540) which contains an imager, a processor and a keypad. Using this system a photographic picture could be taken at 30 to 40,500 frames per second. This system, along with three other components consisting of a computer, a monitor and a video tape recorder, formed the complete setup for photography as shown in Fig. 4. The high-speed photography was operated at 13,500 frames per second and 128×128 resolution. The pictures covered a  $2.5 \times 2.5$  mm cross-section of the visible test section. It was achieved using a 100 mm telephoto lens (SMC PENTAX-M MACRO 1:4 100 mm) with a 180 mm extension tube. The slow motion behavior (10 frames per second) of the bubble was recorded on videotape by the video tape recorder for five minutes for each condition.

For each condition at least 200 consequential images of the bubble behavior were saved in the computer memory. The bubble behavior was visualized for a value range of four variables which included the position along the rod, the inlet subcooled temperature, linear power density and the coolant flow rate.

As indicated in Fig. 3, the rod acceleration was measured using an accelerometer attached to the rod outside the test section.

### IV. EXPERIMENTAL RESULTS

The behavior of bubbles in different conditions of subcooling temperature, linear power density and flow rate was analyzed using high-speed photography. The observed behaviors can be divided into two main categories: a) *general aspects of interfacial behavior of the coolant in subcooled flow boiling and*, b) *specific aspects of bubble behavior at different subcooled flow boiling conditions* which are presented in following:

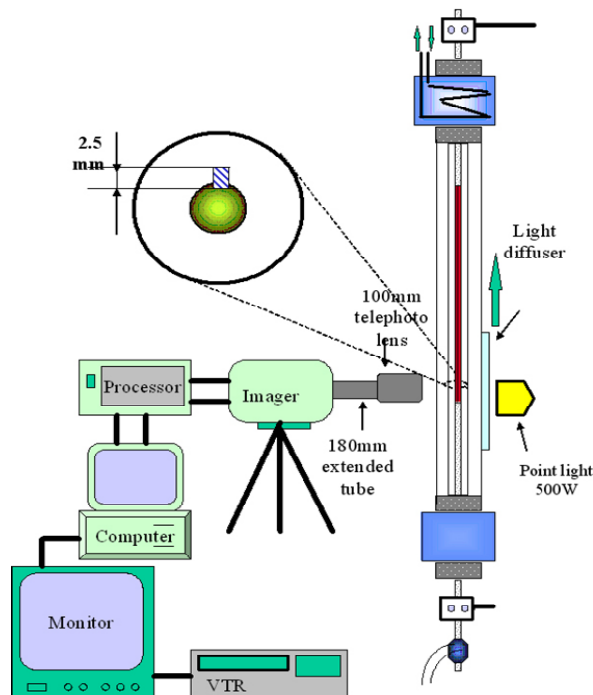


Fig. 4 Experimental setup of high speed photography

#### A. General Aspects

A general bubble behavior in subcooled flow boiling is shown in Fig. 5. In all cases that a bubble formed on the heating surface, a thin shear flow, which looks similar to a dark fluid layer in the photographs, covers the heating surface. This dark layer was expected to be a superheated layer, and therefore, its thickness shows the superheated layer thickness. The darkness of the thin layer can be explained by the difference in the reflection angle of the back light due to the temperature difference between the subcooled water and the saturated or superheated water. This thin layer disappears in linear power densities that are less than those required for the onset of nucleate subcooled flow boiling, and in the low subcooling or in the saturated conditions.

High-speed photography of the bubble ebullition cycle shows that vapor blown from a cavity forms as a bubble with a hemispheric or an elongated hemispheric shape. This process occurs during a short interval between less than 74  $\mu$ s to around 222  $\mu$ s, depending on parameters such as: linear power density, subcooling, and cavity characteristics. The motion of water in the layer around the bubble causes the bubble to separate from the heating surface. The contact area of the bubble with the wall starts to shrink. This continues until the bubble adheres to the wall at a single point, at which time the bubble becomes similar to a balloon. This process is followed by the ejection of the bubble from the surface. Most of the bubble volume condenses in bulk flow near the surface. The collapse starts from the bottom of the bubble. It appears that the condensation rate from the bottom is much more

notable than the bubble top.

Condensation of the bubble and the work due to the surface tension cause a balloon type bubble to change into a micro-bubble with a diameter around one fiftieth of the original bubble. Immediately after its formation, the micro-bubble rapidly escapes from its location towards the bulk flow. A micro-bubble has a relatively high kinetic energy. In addition, a simple theoretical calculation shows that the inside pressure and temperature of a micro-bubble are both relatively high. This state can keep micro-bubbles much more stable than the original bubbles. Due to this stable characteristic of micro-bubbles, the authors call it "stable micro-bubble" or in brief "SMB".

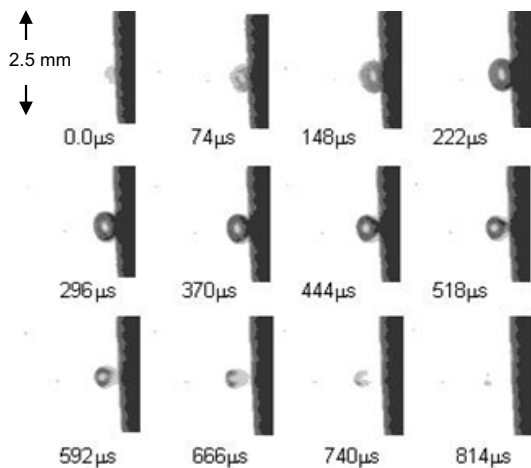


Fig. 5 Typical bubble ebullition cycle in subcooled boiling flow (in heat flux of 100W/cm, liquid subcooling 25K and liquid velocity 0.53m/sec)

### B. Specific Aspects

Several aspects of subcooled boiling and SBIV at different conditions are listed below and summarized in Figs. 6 & 7.

1. The density of active nucleation sites increased with increasing linear power densities and decreasing subcooled temperature.

2. The average bubble maximum diameter decreased with increasing linear power density and subcooled temperature.

3. The bubble emission frequency depends upon the sites. However it increased with increasing linear power density.

4. Bubble growth time varies between 74μs and 222μs. For large bubbles the results show that increasing boiling length and decreasing linear power density, subcooled temperature or the flow rate will slightly increase bubble growth time.

5. Shorter growth time occurred in lower subcooling temperatures and higher linear power densities.

6. Averaged SBIV intensity increased with increasing linear power density and subcooled temperature.

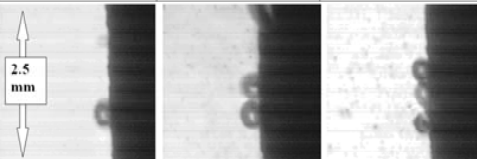
AT <sub>loc,in</sub>	75(K)	50(K)	25(K)
Ave. active sites	↗	↗	↗
Ave. bubble Size	↗	↗	↗
Ave. bubble frequency	↘	↘	↘
Ave. SBIV Intensity	↘	↘	↘
A sample Image			

Fig. 6 A qualitative summary of the subcooled temperature effect on the bubble behavior and the SBIV


LPD	135(W/cm)	182(W/cm)	230(W/cm)
Ave. active sites	↗	↗	↗
Ave. bubble Size at 1cm	↘	↘	↘
Ave. bubble frequency	↗	↗	↗
Ave. SBIV Intensity	↗	↗	↗
A sample Image			

Fig. 7 A qualitative summary of the linear power density effect on the bubble behavior and the SBIV

## V. DISCUSSION

The above results suggest that the following parameters cause a wide range of frequencies of excitation due to the bubble formation and collapse process in subcooled flow boiling on the heating surface.

1) Existence of a large number of cavities on the heating surface with different shapes and sizes,

2) Variation of cavity density and size in different places on the heated rod,

3) Random activation of sites in subcooled boiling, and

4) On-off behavior [15] of the activation sites due to the fluctuation of local surface temperature (because of the moderate thermal conductivity of the stainless steel rod). This characteristic is very important one because it is the main source of fluctuations in boiling parameters locally and occasionally.

Therefore, different excitation frequencies with different energies at different locations cause the rod vibration to exhibit a high power density in the whole range of recorded frequencies during subcooled boiling. This means that SBIV itself does not show any preferred frequency.

Without considering the vibration intensity increase due to the excitation of natural frequencies, the results show an increase in the vibration intensity at higher subcooling temperatures. This observation cannot be fully explained by

the present experimental data. However, the following parameters appear to have some influence on the observed phenomenon.

1) In higher subcooling temperatures bubbles grow and collapse quite rapidly and in proximity to the heating surface (because of the lower lifetime of the bubble). This will cause higher pressure pulses on the heating surface in comparison with those in lower subcooling temperatures.

2) It is found, experimentally, that an explosion in a confined system is more energetic compared to an unconfined system [14]. Since increasing subcooling causes higher surface tension, viscosity and density, the confinement effect of the ambient coolant on the active cavities will increase. Hence, the explosive processes of bubble formation and collapse would result in stronger exciting forces on the heating surface compared to those in low subcooling.

3) The results indicate shorter bubble growth time in higher subcooling (75 K) compared with that in low subcooling (25 K). Therefore, even if the same force would be released from the bubble formation in a cavity, the resulting impact will be stronger in higher subcooling due to the shorter growth time.

#### VI. THE MECHANISM OF EXCITING FORCES ON HEATING SURFACE IN SUBCOOLED FLOW BOILING

Based on the results obtained through high speed photography of the bubble ebullition cycle, the mechanism of the exciting force can be classified into two main categories of bubble-attached region and bubble-detached region. In the following, the discussions on the mechanism of exciting forces on the heating surface are presented in these two categories.

##### A. Forces Acting on the Heating Surface in Bubble Attached Region

As discussed before, the bubble growing process is a highly explosive phenomenon and even for the 2.5mm length of the rod, the bubble growing time somewhat varies from site to site. Furthermore, there are sites that become active or inactivate in different conditions, or even in the same condition due to the on-off behavior of the nucleation sites. Therefore, it would be very difficult to introduce a correlation or equation for the calculation of the forces acting on the heating surface during subcooled boiling based on the results of the present study. However, it would be very useful to have at least a simple quantitative estimate of the forces acting on the heating surface due to bubble formation and collapse. These forces in the bubble-attached region are considered from the view point of the momentum change of the cavity system because of the vapor blown off the cavity. In the following, the force acting on the heating surface due to this process is illustrated. The main parameters for the typical bubbles are listed in Table I.

TABLE I  
A TYPICAL BUBBLE PARAMETERS EXTRACTED FROM THE EXPERIMENTAL RESULTS (LPD182W/CM, SUBCOOLING 75K & FLOW 0.53M/SEC) [10]

Bubble maximum diameter (μm)	Ave. cavity diameter (μm)	Bubble growing time (μs)	Bubble life time (μs)	Force due to ebullition (mN)
125	30	74	148	0.0011
280	40	148	370	0.0217
435	50	148	370	0.2015
555	59	148	500	0.6284
625	70	148	444	0.9042

The pressure difference between the inside and outside of a bubble due to surface tension for a spherical bubble can be calculated from  $\Delta p = p - p_0 = 2\sigma / r$ , where  $p$  and  $p_0$  are, respectively, the inside and outside pressure of the bubble, and  $r$  is the bubble radius. Thus, assuming vapor as an ideal gas, the mass of the vapor in a bubble of radius  $r$  is:

$$m = \frac{\Psi}{RT} \left( p_0 + \frac{2\sigma}{r} \right) \quad (1)$$

where  $\Psi = 4/3\pi r^3$  is the bubble volume, and  $R$  and  $T$  are the vapor gas constant and its temperature, respectively. Then, the rate of change of the bubble mass will be:

$$\dot{m} = \frac{4\pi}{3RT} (3p_0 r^2 + 4\sigma r) \frac{dr}{dt} \quad (2)$$

On the other hand, the average velocity,  $\bar{V}$ , of the vapor discharging from the cavity into the bubble should satisfy the following equation:

$$A_0 \bar{V} = \frac{d\Psi}{dt} \quad (3)$$

Where  $A_0$  is the surface area of the cavity opening. Therefore, the instantaneous average discharge velocity is:

$$\bar{V} = \frac{4\pi}{A_0} r^2 \frac{dr}{dt} \quad (4)$$

Note that evaporation and condensation at the vapor-liquid surface do not affect this balance (Eq. (3)). The reason is that for low heat fluxes, the superheat layer thickness is small, large cavities are activated, and the observed size of the bubble is large. In contrast for high heat fluxes, superheat layer thickness is thick, small cavities are activated, and the size of the bubble is small. Since there is no evidence of having a large bubble in large superheat layer thickness in high power heat fluxes. We did not have small bubble in high power densities with large superheat layer thickness, therefore the affect of the superheat layer evaporation and condensation is not significant.

Thus, the instantaneous force is exerted on the cavity, so on the heating surface, during the bubble growth the process is:

$$F = \dot{m} \bar{V} = \frac{16\pi^2}{3A_0 RT} (3p_0 r + 4\sigma) r^3 \left( \frac{dr}{dt} \right)^2 \quad (5)$$

It is now assumed that the bubble temperature will remain

constant during the bubble growth phase. Furthermore, an average value for the rate of bubble growth,  $\frac{dr}{dt}$ , will be used

based on the typical quantities obtained from experimental observations. Therefore, integrating Eq. (5), the average force exerted on the heating surface during the growth phase for a typical bubble will be:

$$\bar{F} = \frac{16\pi^2}{3A_0RT} \left( \frac{dr}{dt} \right)_{\text{ave}}^2 \left[ 0.6p_0 \frac{(r_{\text{max}}^5 - r_0^5)}{r_{\text{max}} - r_0} + \sigma \frac{(r_{\text{max}}^4 - r_0^4)}{(r_{\text{max}} - r_0)} \right] \quad (6)$$

Where  $r_0$  and  $r_{\text{max}}$  are the initial and maximum radius of the bubble, respectively. Here, we take  $r_0$  equal to the radius of the cavity opening, and  $A_0 = \pi r_0^2$ .

Based on a value of  $\sigma = 0.074$  N/m for water at 20°C and 1 bar, and the values given in Table I, the average force,  $\bar{F}$ , is calculated and the results indicate that the formation of a typical bubble in subcooled boiling is predicted to exert an excitation force in the order of  $10^{-4}$  N.

Fig. 8 shows exerted force on the heating surface during the bubble growth process versus bubble diameter. It can be seen that the exerting force on the heating surface increases as the bubble diameter increases.

Although the above calculations are very simple, a rough quantitative estimate of the exerted force during this phase is obtained. This value can, at least, give us the order of magnitude of the average force which is partially responsible for SBIV due to the bubble formation and growth phase. In the present experiments, no attempt was made to measure the exerted force on the rod, and therefore, no co-relation between the estimated force and the actual force can be established.

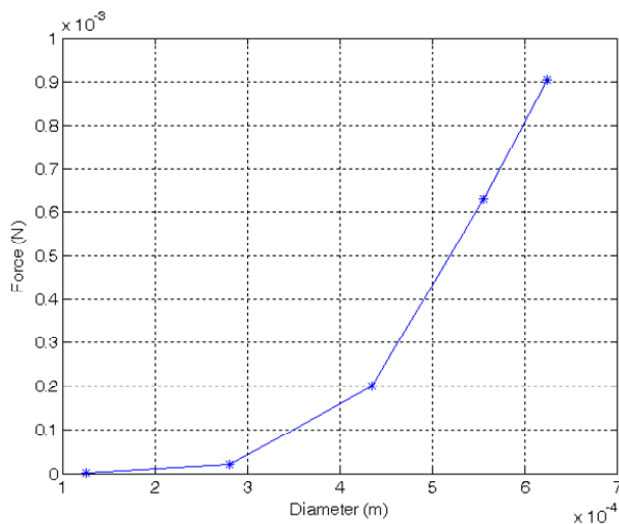


Fig. 8 Exerted force on the heating surface during the bubble growth process versus bubble diameter for the tabulated experimental data in Table I

### B. Forces Acting on the Heating Surface in Bubble-Detached Region

In the equation (6) the quantitative role of surface tension is

not remarkable; therefore, the variation of the surface tension due to subcooling itself can not explain the observed increasing of the SBIV intensity with the subcooling temperature. However, it could be conclude that the collapse process in bubble-detached region that would have more significant role regarding to the bulk flow subcooling and it play the main role in SBIV.

After bubble detachment, the collapse process occurs from the bottom of the bubble near the heating surface in high subcooling conditions. The proximity of the bubble collapse location to the heating surface can cause a force effect on the surface in two ways. One mechanism is due to the pressure pulse generated during the bubble collapse process, and the other is due to the rush of water around the detaching bubble against the heating surface; the latter acts as a water hammer phenomenon on the surface. Based on the experimental evidence (high speed photography) it is suggested that the collapse process occurs in a longer time interval compared with that for bubble growth. However, induced forces due to collapse are not calculated in the present work and this could have an effective force due to vapor and water movement. Actually, the collapse process involves the motion of water, which has a density two or three order greater than vapor density. Therefore, the calculation of the force due to the bubble collapse remains as an interesting subject to challenge.

As discussed before, the product of a collapsed bubble is a micro-bubble that it is more stable compared to the original bubble. The stable micro-bubbles have no influence on SBIV, since they form at the final stage of the bubble collapse process when the bubble has significantly condensed and reached a relatively stable state.

## VII. CONCLUSION

The most important conclusions of the present study on the vibration mechanism of a heated rod due to subcooled flow boiling are listed in the following.

1. Interfacial study of a coolant with a heating surface was carried out by high-speed photography. Hence, bubble behavior in different conditions of subcooled boiling was used to explain some aspects of SBIV.

2. The bubble behavior during a bubble ebullition cycle in subcooled conditions is illustrated. The results indicate that the collapse process starts from the bottom of the bubble after bubble detachment from the heating surface in the all of persented subcooling conditions.

3. In the present study, a model based on surface tension and momentum transfer was introduced to estimate the order of magnitude of the force exerted on the heating surface due to bubble formation. This indicates that the formation of a bubble in subcooled boiling can cause a force of the order  $10^{-4}$  N per bubble on the heating surface.

4. Induced forces due to the collapse process are not calculated in the present work and this could have an effective force due to vapor and water movement. Also, we used a quasi-static model of bubble growth for the presented model.



However, according to the mentioned references this model gives a pressure difference lower than the unsteady state that was actually expected during the bubble growth. Therefore, for this reason, in our model, a lower force limit due to the bubble ebullition in subcooled flow boiling is evaluated and calculation of the force due to the bubble collapse remain as an interesting subject to challenge.

5. This article is just a starting point for calculating the force induced by SBIV and the following subjects are interesting for future research works:

i) Development of a suitable model to evaluate the effect of unsteady-state conditions

ii) A model to evaluate the induced forces due to the collapse process.

iii) Vibrational analysis of a heated rod under subcooled boiling condition regarding forces acting on the surface

iv) Evaluation of the magnitude of the overall resulting force induced by SBIV on the rod, by a statistical approach accounting for active nucleation site distribution then it could clearly illustrated that, how could be possible that SBIV may induce sensible vibrations and how to prevent the exaltation of natural frequency in those systems that may works under subcooled boiling condition?

#### ACKNOWLEDGMENT

The experimental facility for this investigation was provided by Advanced Fusion Reactor Engineering Laboratory of the Department of Quantum Science and Engineering of Tohoku University, Japan. Inspiring discussions with Prof. Toda and Prof. Hashizume are also acknowledged.

#### REFERENCES

- [1] Omatskii, A.P. and Vinyarskii, L.S., 1965, "Critical Heat Transfer in the Forced Motion of Under heated Water-Alcohol Mixtures in Tubes of Diameter 0.5mm", *Teplofizika Vyskikh Temperature (High Temperature)*, Vol. 3, No. 6, pp. 881-3.
- [2] Zhou Tao, Wang Zenghui, Yang Ruichang, 2005, "Study on model of onset of nucleate boiling in natural circulation with subcooled boiling using unascertained mathematics", in *Nuclear Eng. And Design*.
- [3] Sakurai, A., 2000, "Mechanisms of transitions to film boiling at CHF in subcooled and pressurized liquids due to steady and increasing heat inputs", in *Nuclear Eng. And Design*.
- [4] Nematollahi, M.R., Toda, S. and Hashizume H., 1998, "Characteristic Phenomena of Subcooled flow boiling Instability", *Proceeding of the 6th Int. Conference on Nuclear Engineering (ICONE6)*, Paper No. 6403.
- [5] Nematollahi, M.R., Toda, S. and Hashizume, H., 1998, "Vibration Characteristic of Subcooled flow boiling Instability", *1st European-Japanese Two-Phase flow Group Meeting, and 36th European Two-Phase flow Group Meeting, Portoroz, Slovenia Jun 1-5*.
- [6] Nematollahi, M.R., Toda, S., Hashizume, H. and Yuki, K., 1999, "Vibration Characteristic of Heated Rod induced by Subcooled flow boiling", *Journal of Nuclear Science and Technology*, Vol. 36, No. 7, pp. 575-583.
- [7] Bergles, A.E., 1964, "In Influence of Flow Vibration on Forced-Convection Heat Transfer", *Transaction of the ASME, J. of Heat Transfer*, Vol. 107, pp. 559-560.
- [8] Takahashi, K. and Endoh, K., 1990, "A New Correlation Method for the Effect of Vibration on Forced-Convection Heat Transfer", *J. of Chemical Engineering of Japan*, Vol. 23, pp. 45-50.
- [9] Smimov, H.F., Zrodnikov, V.V. and Boshkova, I.L., 1997, "Thermoacoustic Phenomena at Boiling Subcooled Liquid in Channels", *Int. J. Heat & Mass Transfer*, Vol. 40, No. 8, pp. 1977-1983.
- [10] Celata, G.P., Dell Orco, G. and Gaspari, G.P., 1995, "Detection of Subcooled Boiling Heat Transfer Regimes up to Critical Heat Flux by Acceleration Equipment", *Fusion Engineering and Design*, Vol. 28, pp. 44-52.
- [11] Nematollahi, M.R., Hashizume, H., and Toda, S., 1998, "The Heated Rod Vibration in Different Heat Transfer Regimes", *1998 Fall Meeting of the Atomic Energy Society of Japan*, Paper No: G16, pp.410.
- [12] Nematollahi, M.R., 1999, "Fundamental Study of Vibration Induced by Subcooled flow boiling", *Ph.D. thesis, Tohoku University, Japan*.
- [13] Toda, S., and Nematollahi, M.R., 2000, "Heat Transfer Mechanism of Subcooled flow boiling According to High-speed Photography Results of a Heating Surface", *Second Japanese-European Two-Phase Flow Group Meeting, September 25-29, Tsukuba, Japan*.
- [14] Rinehart J.S. and Pearson J., 1963, "Explosive working of metals", Oxford, Pergamon Press.
- [15] Del Valle M.V.H. and Kenning D.B.R., 1985, "Subcooled flow boiling at High Heat Flux", *Int. J. Heat & Mass Transfer*, Vol. 28, pp. 1907-1920.